Structural Health Monitoring for Life Management of Aircraft

Qiaojian Huang, Brad Regez and Sridhar Krishnaswamy

Center for Quality Engineering and Failure Prevention,

Northwestern University, Evanston, IL 60208, USA

ABSTRACT

In this paper, the influence of disbond damage on Lamb wave propagation in GLAss-REinforced (GLARE) composites is described. A finite element method (FEM) model was constructed to simulate the influence of a disbond defect on the lamb wave propagation in a GLARE laminate. Both the displacement amplitudes and travel time of the A_o mode Lamb wave were shown to be influenced by the disbond void. In experiments, a disbond defect was introduced with ball drop test to study their influence on the Lamb wave signals. Modally-selective guided Lamb waves were demonstrated to be launched successfully and were used to detect the disbond defect in the GLARE plate. The measured A_0 mode Lamb wave signals were found to decay exponentially with increasing the disbond diameter which was measured with a thermal imaging technique. It is shown that the disbond defect sizes can be predicted from the measured Lamb wave signals using the exponential model.

Keywords: Disbond defect, Lamb waves, Finite element method (FEM), Ball drop test, PVDF transducer

1. INTRODUCTION

GLAss-REinforced (GLARE) laminate is a new class of fiber metal laminates (FML), which are hybrid composites consisting of thin alternating bonded layers of metal sheets and fiber-reinforced epoxy prepreg [1]. The GLARE composites possess excellent properties from the combination of metals and fibrous composite materials [2]. For that reason, the GLARE composites offer outstanding fatigue resistance, excellent impact resistance, and fire resistance, etc [2]. The most attractive property is at least 20% weight reduction while exhibiting superior material properties, compared with the traditional aluminum alloy used in the aerospace industry [3]. Consequently, the GLARE composites have been used in a substantial part of the fuselage in aircraft such as Airbus 380 [4, 5].

Disbond defects are a matter of serious concern in safety-critical aerospace composite parts in service [6]. Guided Lamb wave techniques have shown great potential for both quantitative non-destructive evaluation (QNDE) and SHM applications owing to their large area inspection capability [7, 8]. Therefore, the assessment of the influence of the disbond defect on the Lamb wave propagation is significant. One objective of this work is to theoretically study the interaction of A_o-mode Lamb wave with a disbond void in a GLARE plate.

Structural degradation, whether engendered by inherent material aging due to the environment and service loads (fatigue, corrosion etc) or by unpredictable external events (impact etc), is an inevitable part of life. Intelligent Structural Health Management (ISHM) systems are needed to predict structural failure of safety-critical structures, such as airplanes, which are not allowed to fail in service. In the past, ball drop induced delamination in the GLARE composites has been reported and correlated to various factors

including impact energy [9, 10], impact events [9, 11], and material post-curing effect [11]. Another objective of this work is to demonstrate an application of Lamb wave technique in monitoring the growth of the impact disbond defect in adhesive-bonded composites,

In this paper, the effect of the disbond defects on the Lamb wave propagation in a GLARE plate will be explored theoretically and experimentally. The theoretical investigation is conducted with finite element method (FEM). A series of experiments are introduced on guided Lamb wave generation and detection, ball drop induced disbond defects, and a thermal imaging technique. The relationship between the disbond defect size and the detected Lamb wave amplitudes will be ascertained from the experimental results. We demonstrate that modally selective Lamb waves can be effectively used to detect impact damage and estimate disbond defect size in the GLARE composite.

2. EXPERIMENTS

GLARE 2A-2/1-0.4 was selected for our experimental tests. The GLARE plate consisted of two layers of aluminum alloys (0.4mm in thickness) and one layer of glass fiber/epoxy prepreg (0.25mm thick) forming a sandwich structure. The prepreg orientation in each fiber layer is 0/0. The GLARE plate was purchased from FMLC (Fibre Metal Laminates Center of Competence) in the Netherlands, where the GLARE composites were invented.

2.1 Lamb-wave Test

Polyvinylidene fluoride (PVDF) film, provided by Measurement Specialties, Inc., was used as the piezoelectric media for Lamb wave transducers. The PVDF film is thin (110 μm) and flexible, which produces malleable sensors with a low profile and low cost. The

PVDF film was attached to the GLARE plate with M-Bond 200 and copper comb electrodes were mounted. Both the transmitter and the receiver have the same electrode configurations. Each transducer has 10 electrode fingers with the finger length of 20 mm and the spacing of 2.45mm. One of the transducers was used to launch Lamb waves and the other one was to detect the signals across the surface of the plate. The distance between the two PVDF transducers is 200 .

Figure 1 shows an examination system for Lamb wave test on the GLARE composite material. Ten cycles of a Hanning windowed tone burst signal were generated from a function generator with the form of:

$$V(t) = \begin{cases} \frac{V_o}{2}[1 - \cos(2\pi f_0 t / n_0)]\cos(2\pi f_0 t), & t \le n_0 / f_0 \\ 0, & t > n_0 / f_0, \end{cases} \quad (1)$$

where V_0 = 250 mV is the peak-to-peak voltage, f_o = 695 KHz is the central frequency and n_o =10 is the number of the sinusoidal cycles within the Hanning window. The excitation signal was amplified by a RF amplifier (G=377) before applying to the electrodes of the PVDF transmitter and generating Lamb waves in the GLARE plate. The Lamb wave signals were picked up by the PVDF receiver and a signal conditioner was applied before being recorded by a digital oscilloscope. An active 3-pole low-pass filter was built to filter out noise and to suppress undesired modes of Lamb wave signals. The cut-off frequency of the filter was set to ~1 MHz with a roll-off slope of -60 dB/decade. The filtered Lamb wave signals were amplified by a pre-amp with a gain of 34 dB.

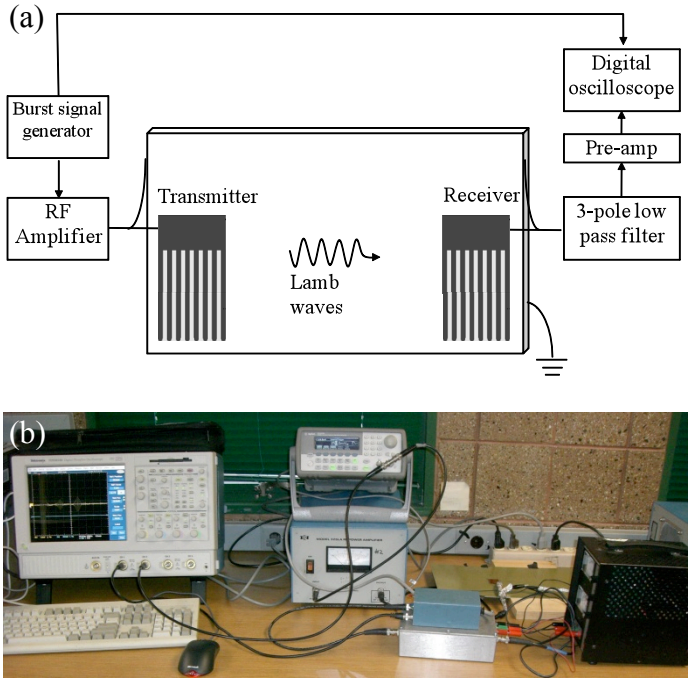

Figure 1: An examination system for Lamb wave test: (a) system schematic and (b) experimental setup.

2.2 Ball Drop Test

A ball drop was used to introduce disbond defects in the GLARE plate. The ball drop test was carried out by releasing a 1-inch diameter steel ball from 3-feet height to strike the center point of the GLARE plate between the two PVDF comb transducers. The impact energy is 606 mJ converted from the kinetic energy of the falling ball. The impact events ranged from 0 to 200 times. After each ball-drop test, the experimental system for Lamb wave measurement was used to study the influence of ball drops on the detected Lamb wave signals.

2.3 Thermal Imaging Technique

After each ball-drop test, the GLARE plate was examined with using a pulsed thermography system in reflection mode. Figure 2 shows the inspection system for thermal

imaging of the GLARE composite material. Two flash lamps were used to irradiate the sample surface to generate a temperature gradient in the GLARE plate. Thermal images were taken in time sequence starting just before the pulsed light irradiation and ending some time after to include temperature-dependent phenomena. The acquisition rate was 50 Hz with a full frame size of 640 × 512 pixel. A thin layer of washable black paint was applied on the GLARE sample surface to help the light absorption.

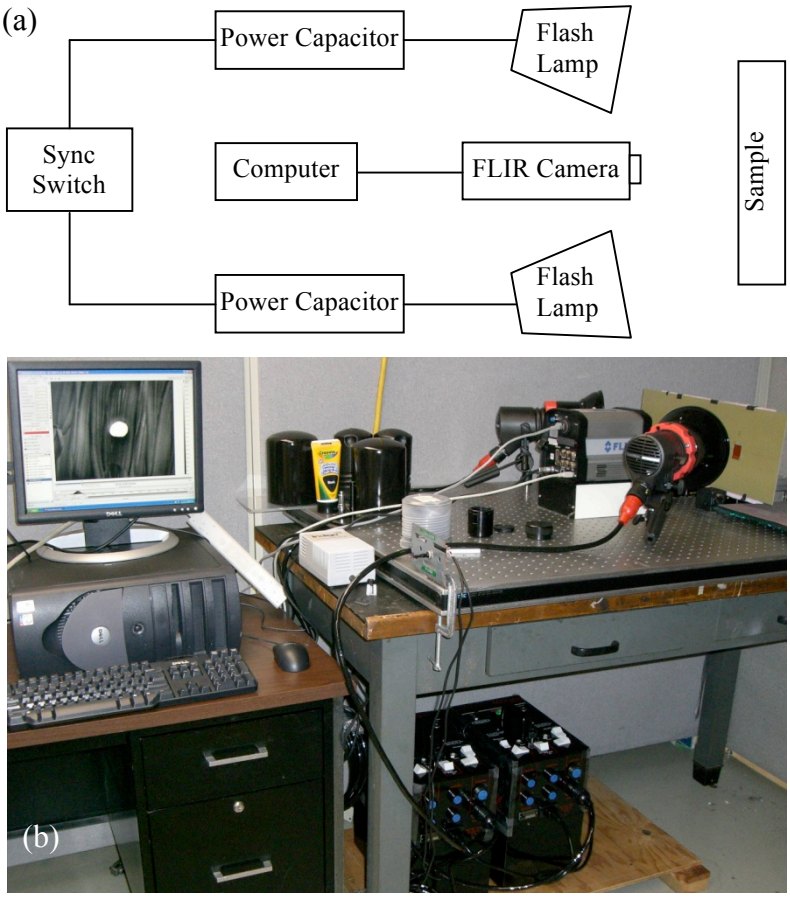

Figure 2: An inspection system for thermal imaging:(a) system schematic and (b) experimental setup.

3. THEORY

3.1 FEM Model on Lamb Wave Simulations

As indicated by Petculescu et al. [12], modally-selective transducers can be used effectively as SHM tools to monitor the size of disbonds. To investigate the design parameters for such sensors, a finite element model was constructed to investigate the influence of disbonds on the Lamb wave propagation in the GLARE plate. Computations were made with the commercial software, ANSYS. As shown in Figure 3, Lamb waves were launched with a PVDF film by applying tone-bust voltages on the piezoelectric film with a 10-finger comb pattern. The layer thicknesses of the GLARE plate were based on the product dimensions. The PVDF film thickness is 110 μm, which is the typical thickness available from commercial vendors. The length of the GLARE plate in the FEM model is 400 mm. The spacing of the tone-burst voltage is 2.45 mm which matches the wavelength of the A_o mode Lamb wave. There are at least 20 nodes per wavelength and a full transient analysis was done with the integration time steps of ~1-4×10^{-8} s. The selected time step satisfies the optimum value of less than the travel time of Lamb waves in an element size for the studied frequency. Plane 13 (2-D structural solid) and Plane 42 (2-D coupled-field solid) were selected as elements for PVDF film and the GLARE plate, respectively.

In order to launch narrow-band Lamb waves in the GLARE plate, the excitation sinusoidal signal with Hanning window, as Equation (1), was applied on the top surface of PVDF film. In this FEM model, V_o = 400 V, f_o = 950 KHz, and n_o = 5. From symmetry, only half of the plate is modeled by applying symmetry boundary condition for the *x*-

displacement, U_x, at x = 0. The bottom surface of the PVDF film was electrically grounded by applying 0 V to the nodes at the interface between PVDF film and the Al alloy layer.

The influence of a disbond void on the Lamb wave propagation was studied by creating a void in the Fiber/epoxy layer. The disbond void is located at x = 100 mm. The length of the disbond varies from 0.1-4.0 mm while keeping a constant height of 0.25 mm which is the thickness of the Fiber/epoxy layer. The displacement of the propagated Lamb wave was monitored on the top surface of the GLARE plate at x = 200 mm.

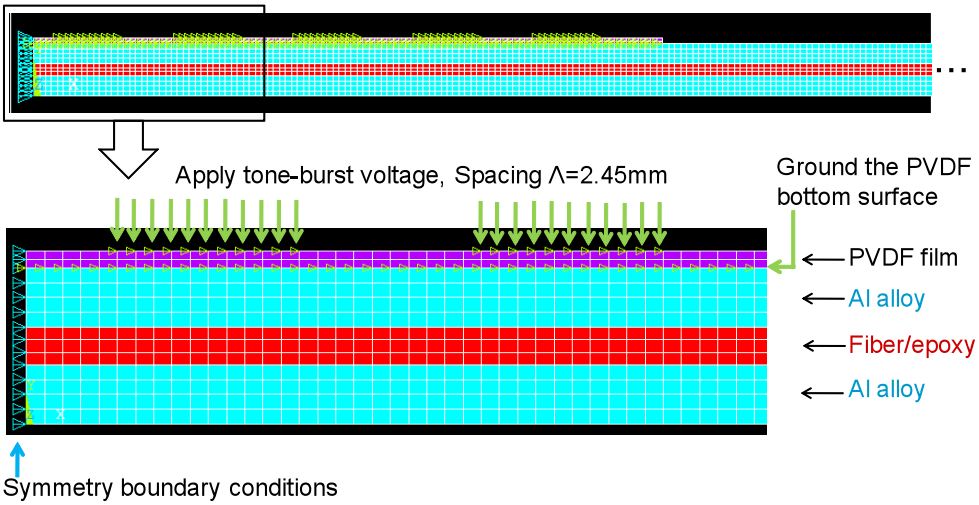

Figure 3: A schematic setup of the FEM model for the Lamb wave simulations

3.2 Influence of a Disbond Void on the Lamb Wave Propagation

Figure 4 shows the displacement components, U_x and U_y, on the top surface of the GLARE plate at x = 200 mm for various void sizes at x = 100 mm. Black curves show the Lamb wave propagation for the GLARE plate without a disbond void. As can be seen, A_o mode Lamb wave was successfully launched with the PVDF comb transducer in the FEM model and the propagation of Lamb waves is clearly indicated. S_o mode Lamb wave with

much smaller amplitudes was also present in the FEM model as shown in Figure 4, which is inevitable for the narrow-band launching signal and the limited width of the comb transducer in the FEM simulations.

As shown in Figure 4, the effect of five different disbond sizes was compared on the Lamb wave propagation in the GLARE plate: 0.1mm×0.25mm (Red), 0.5mm×0.25mm (Green), 1.0mm×0.25mm (Blue), 2.0mm×0.25mm (Pink), and 4.0mm×0.25mm (Cyan) in length × height of the disbond void. The amplitudes of displacement components for the A_o mode lamb wave decrease with increasing disbond length from 0.1 mm to 1.0 mm. However, this trend reversed for the void length larger than 1.0mm. The smaller displacement amplitudes in the A_o mode Lamb wave are attributed to the reflection and scattering of the Lamb wave by the disbond. Additionally, there is an oscillation tail in the Lamb wave displacements for the void size of 2.0mm×0.25mm. A certain void size can result in the oscillation tail in the A_o mode Lamb wave displacements. The oscillation tail can be attributed to the multi-reflections of Lamb waves in the void region and thus the disbond void behaves like a ‘resonator’ generating an exponential decayed Lamb waves.

In addition to the influence on the displacement amplitudes, there is time delay for the A_o mode Lamb wave propagating through the disbond void of various sizes. As the Lamb wave reaches the disbond area where the void separates the GLARE plate in two symmetric sections (Al alloy layers) with less than half of the whole plate thickness, the Lamb wave is forced to propagate through the two adjoining sections. The lower phase velocity of the A_o mode Lamb wave propagating in the disbond region results in the time delay at the monitored spot. Therefore, the travel time of the A_o mode Lamb wave increases with increasing the void length. Both the influence of the disbond void on the

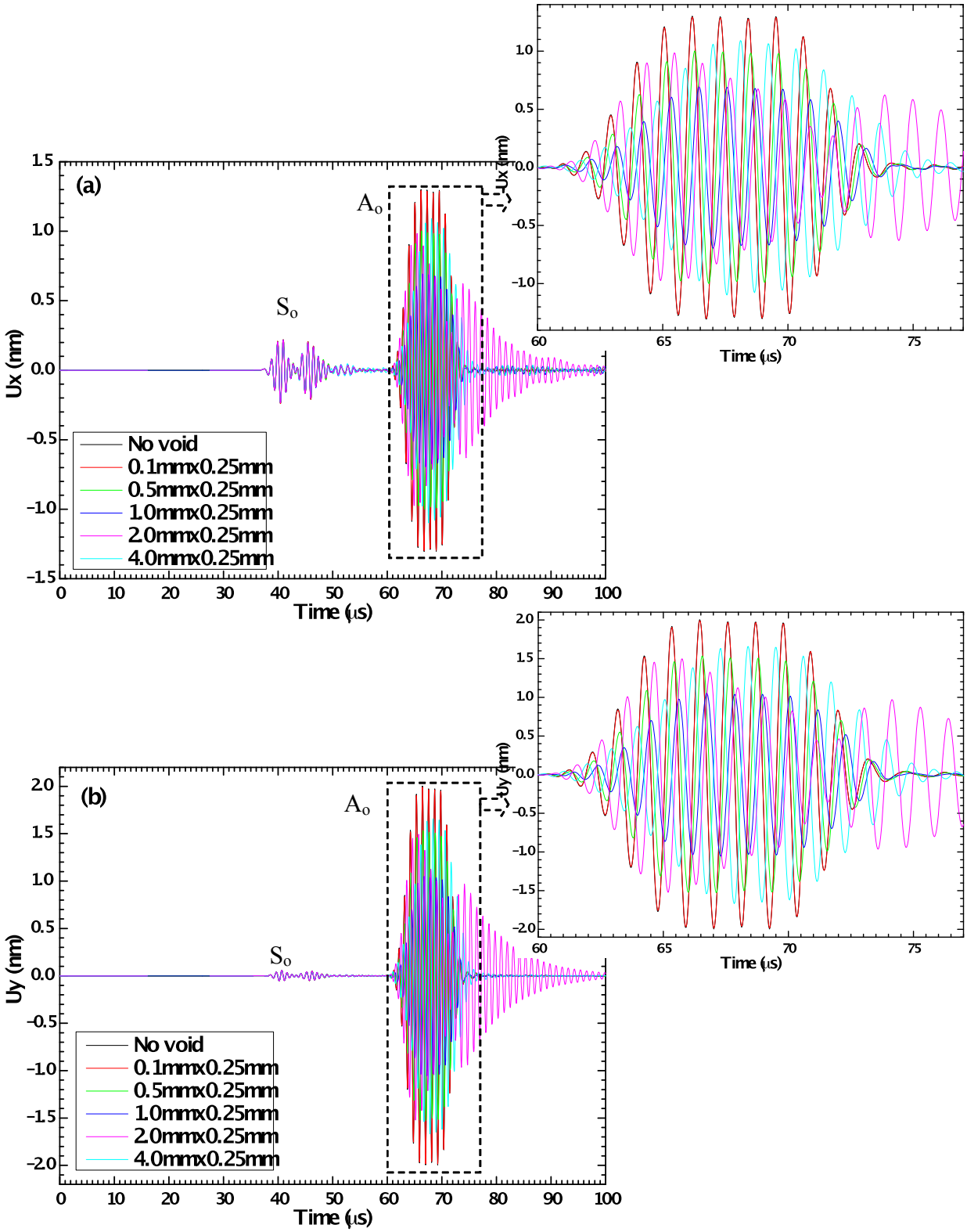

Figure 4: Displacement component of (a) U_x and (b) U_y monitored at x=200mm on the top surface of the GLARE plate with a disbond void (x=100mm) of various sizes

displacement amplitudes and the travel time of A_o mode lamb wave can be clearly observed from the insets of Figure 4. This is consistent with the results of Petculescu *et al* [12], and indicate that time-delay measurements can serve as a basis for the development of SHM sensors for online monitoring of disbond growth.

As an example, the quantitative influence of a disbond void on the A_o mode Lamb wave (U_y component) is summarized in Table 1. There is a negligible effect on the Lamb wave displacement when the disbond void is of 0.1 mm × 0.25 mm in size. The influence is less than 1% on the reduced displacement amplitudes. However, the influence of the disbond void becomes significantly more important in determining the A_o mode Lamb wave amplitudes as its size increases. For instance, the percentage of the reduced displacement amplitudes reaches ~47% as the void length increases to 1.0 mm.

Table 1: Amplitudes and travel time of the displacement component (U_y) of the A_0 mode Lamb wave versus void sizes

Void length (mm)	Void height (mm)	U_y maximum amplitude (nm)	Percentage of U_y maximum amplitude	Arrival time of the first U_y peak (ms)	Time delay in U_y (ms)
0	0	2.00	--	61.23	--
0.1	0.25	1.99	99.5%	61.23	0
0.5	0.25	1.53	76.5%	61.29	0.06
1.0	0.25	1.05	52.5%	61.44	0.21
2.0	0.25	1.50	75.0%	61.56	0.33
4.0	0.25	1.65	82.5%	61.98	0.75

The travel time of the first peak of the A_o mode Lamb waves (U_y component) was traced for the GLARE plate with and without the disbond void of various sizes in Table 1. There is no measurable time delay when the disbond void size is less or equal to 0.1 mm × 0.25 mm. However, the time delay increases from 0.06 μs to 0.75 μs when the disbond lengths increase from 0.5 mm to 4.0 mm. These results imply that the A_o mode Lamb wave signal is very sensitive to the disbond void and can be used for the structural health monitoring of adhesively-bonded composites. The resolution of the disbond detection can be as small as 0.1 mm with the A_o mode Lamb wave at the selected frequency.

4. RESULTS AND DISCUSSION

4.1 Influence of Ball-drop Impacts on the Lamb Wave Test

As shown in Figure 5, guided Lamb waves were demonstrated to be launched successfully and were used to study the influence of the disbond defect on the A_0 mode Lamb wave signals at 695 KHz. Figure 5 (a) shows the launching signal of ten cycles of the tone-burst waveform generated with a function generator. The black curve in Figure 5 (b) is the detected signal for the pristine condition of the GLARE. The signals at the very beginning of Figure 5(b) are the electrical coupling from the emission of the excitation source. It is also noted that there is a group of weak signals between 40 μs and 60 μs. The first part of this group of signals appears to be the S_o mode since its velocity is estimated to be close to the theoretical expectation. The second part of this group of signals has a frequency of ~2.2 MHz, which is about 3 times of the launching signal frequency. These are likely to be from the A_1 or S_1 modes although they are not intended to be launched by our

transducer. Figure 5(b) also shows the detected Lamb wave signals collected for various impact events of 20~200 times.

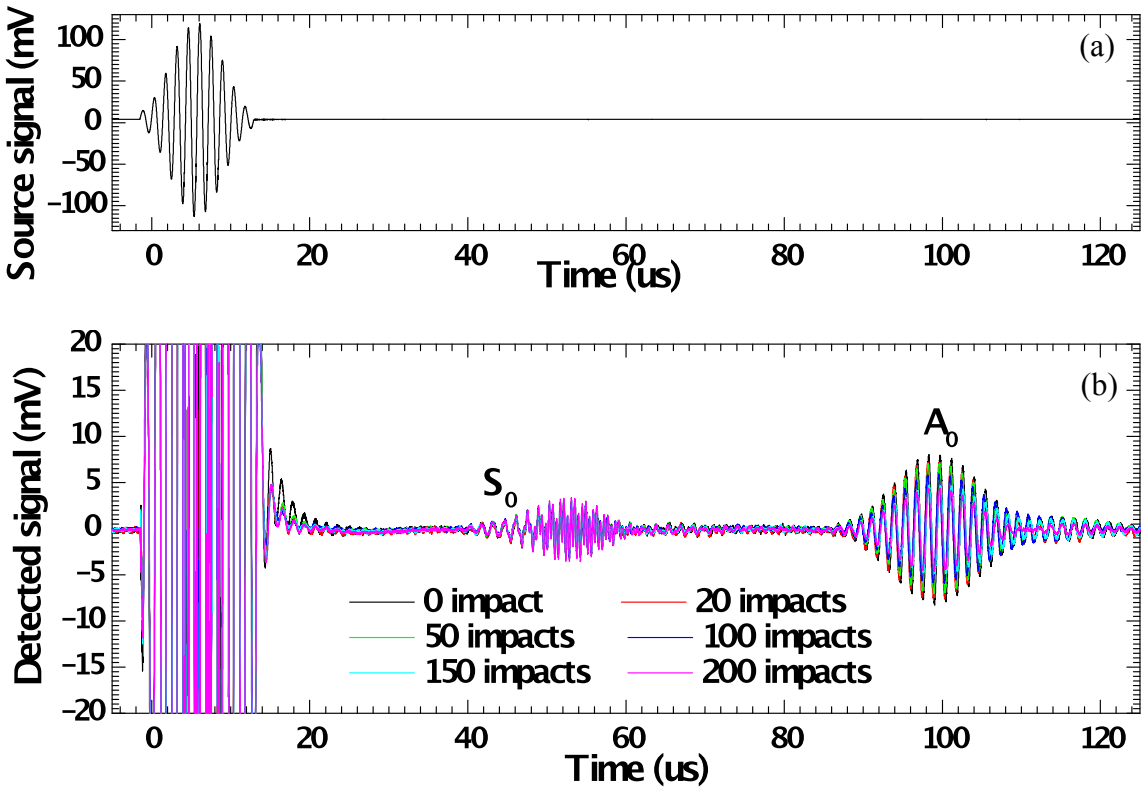

Figure 5: Lamb wave testing at *f* = 695 KHz: (a) Launching signal, (b) Detected signal for various ball impacts.

Figure 6 (a) shows the detected A_0 mode Lamb wave signals for various ball impacts. As can be seen, the measured A_0 mode Lamb wave signals decrease as increasing the ball impact events. The maximum peak-to-valley voltages of the detected A_0 mode Lamb waves can be obtained for various impact numbers, which are plotted in Figure 6 (b). A linear fit was used to fit the experimental data with the least square method. The linear relationship between the detected A_0 mode Lamb wave amplitudes and the number of impacts is indicated from the good correlation coefficient (*R*=-0.984). The closer the

coefficient is to −1, the stronger the correlation between the experimental data and the fitting line.

It is note that the detected A_0 mode Lamb waves arrive almost at the same time for various impact events. There is no apparent time delay or a consistent trend on the travel time of the selected A_0 mode Lamb wave with increasing the number of impacts. In the previous research work in our group, Petculescu *et al.*, reported that time delay grows steadily as the impact damage accumulates on a carbon-epoxy cross-ply composite panel [12]. They attributed the time delay to the lower effective material stiffness induced by the continuous impacts, which results in a lower velocity and therefore an increasing of time delay. The discrepancy between the two experimental results could be attributed to the different structure of the composite materials.

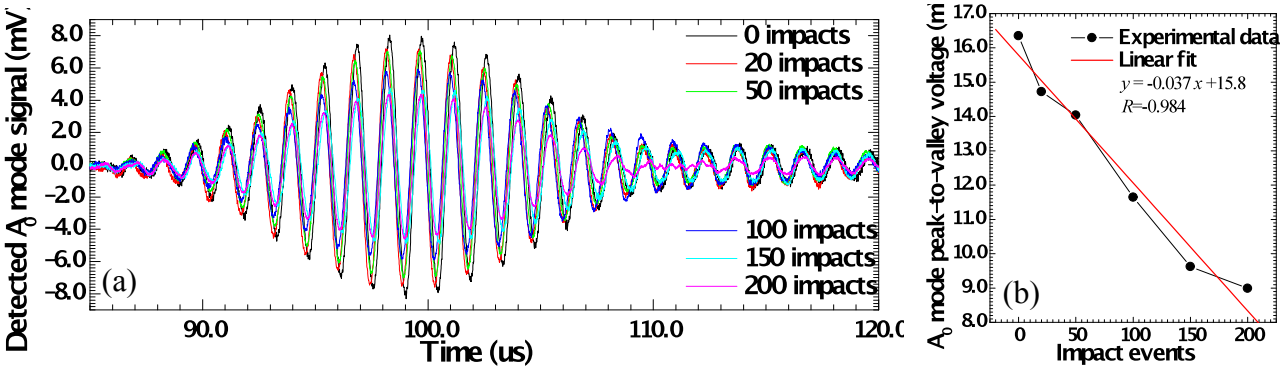

Figure 6: (a) Detected A_0 mode Lamb wave signal for various ball impacts; (b) The influence of the ball impacts on the A_0 mode Lamb wave maximum peak-to-valley voltages.

The previous FEM model predicted that both the displacement amplitudes and travel time of the A_o mode Lamb wave were shown to be influenced by a disbond void. The travel time of the A_o mode Lamb wave increases as the disbond size increases. Our experiments,

however, shows no trace of consistent time delay tested in the GLARE composite. The discrepancy between the theory and experiment could be due to the fact that the modeled 'disbond void' cannot perfectly represent the actual disbond defect. The ball impact involves not only delaminations at the interfaces, but also damage of the glass fiber and matrix. Another reason could be ascribed to the fact that the damage defect diameter is smaller than the of the finger length of the PVDF comb transducer. One may suspect that the reduced amplitude with the ball impact could be caused by the disbond between the transducers and the GLARE plate. However, this possibility can be excluded by observing the detected signals between 40 μs to 60 μs in Figure 5. The amplitudes of this portion of signals are actually enhanced, instead of reduced, with increasing the number of impacts. The most likely change in amplitude is therefore mode-conversion from the A_o mode to higher modes.

4.2 Disbond Defects Induced by a Ball Drop

The disbond defect was further confirmed and measured with a thermal imaging system. An active thermal imaging technique was achieved with the application of an external light heating source to stimulate heat flow within the GLARE plate while the surface was monitored for spatial temperature variations as it returns to thermal equilibrium. As an example, Figure 7 shows the thermal images of the disbond defect area for (a) 100 times, (b) 150 times, and (c) 200 times of ball impacts. These pictures were captured at 0.02s after triggering the flash lamps. The black area is the undamaged GLARE plate and the white spots in the center are the induced disbond defects. The smaller thermal conductivity and its discontinuity around the disbond defect region leads to a higher temperature on the corresponding monitored surface. Therefore, the 'hot' area

(white in the thermal images) represents the disbond defect in the glass fiber epoxy layer. These spatial variations can be an indication of internal flaws, such as disbond defects, that tend to increase the thermal impedance of the structure. The enhanced thermal impedance due to the disbond defect can result in localized surface temperature differentials up to a few tens of Kelvins. Note that although there are some traces left on the black area which are caused by the non-uniform ink painting, the overall information about the disbond defect can still be clearly acquired for the size measurement.

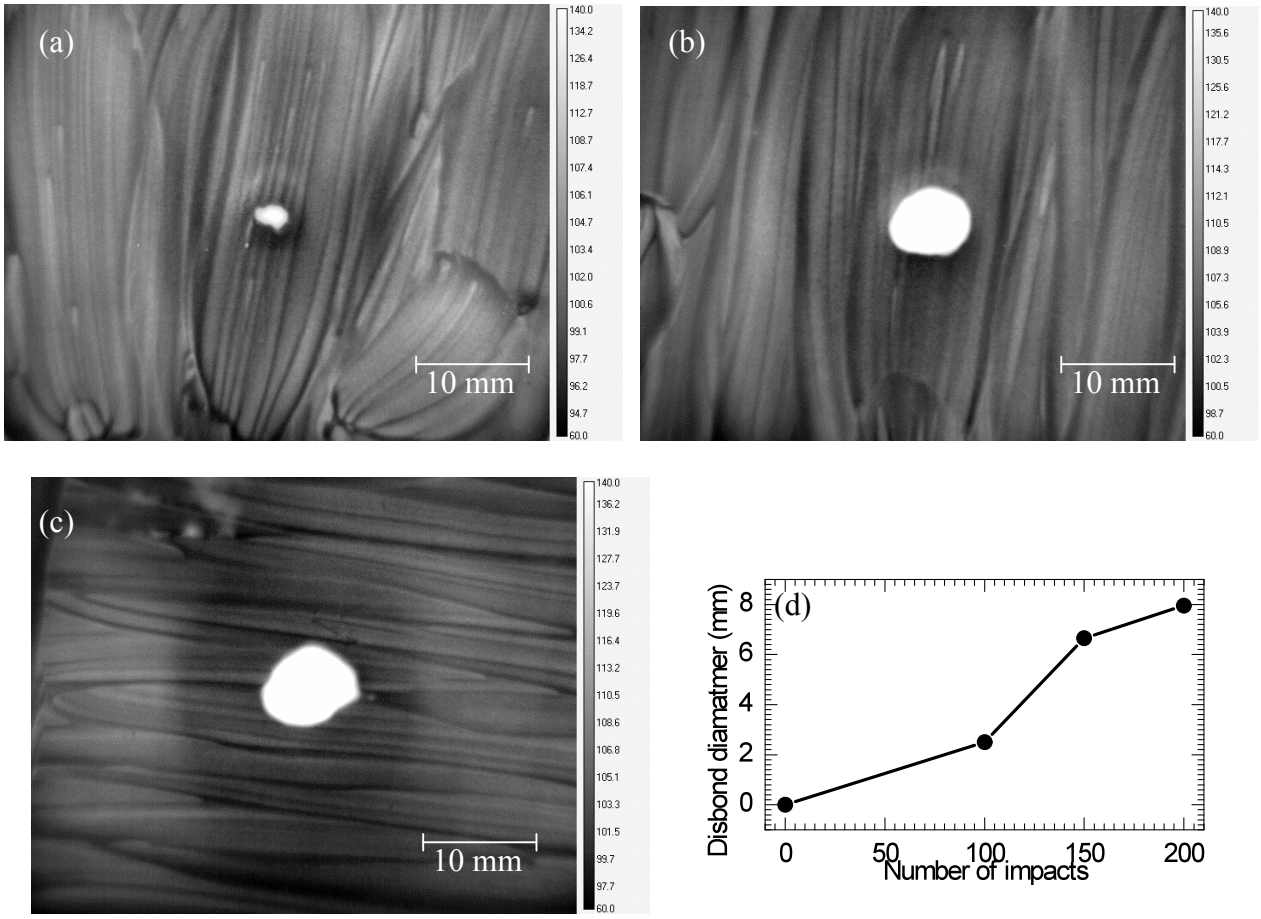

Figure 7: Thermal images of the single-sided inspection on the disbond defect with various numbers of impacts at 606 mJ for (a) 100 times, (b) 150 times, and (c) 200 times. The disbond defect size growth is shown in (d).

As shown in Figure 7 (d), the size of the disbond defect was measured by comparing the pixels of the thermal images for the disbond defects and a ruler placed on the GLARE plate surface. As expected, the disbond defect diameter increases with increasing number of impacts. It is worth to note that the disbond defects of 50 or less ball impacts is not detectable with the thermal imaging system. As a comparison on the sensitivity to the disbond defects, the Lamb wave A_0 mode amplitude is more sensitive to the ball impacts. As shown in Figure 6 (b), the Lamb wave detection shows 10.0% decrease in A_0 mode amplitude after 20 times of ball impacts. Therefore, Lamb wave examination has proven to be efficient on disbond defects, especially for the *in-situ* structural health morning (SHM) application.

Figure 8 shows the percentage of the measured A_0 mode Lamb wave signal reduces with increasing disbond defect diameter. The reduced A_0 mode amplitudes can be attributed to wave reflection [13], scattering [14], and mode conversion in the disbond defect area. The mode conversion in the disbond defect region can be further confirmed from the collected signals between 40 μs to 60 μs in Figure 5. The amplitudes in this time interval increase with increasing the number of impacts. A first order exponential decay was used to fit the percentage of the measured A_0 mode Lamb wave voltage versus the disbond defect diameter. The equation can be expressed as:

$$y = \exp(-x / D_0) \tag{2}$$

where y is the percentage of the measured A_0 mode Lamb wave voltage and x is the disbond defect diameter. The best least square fit is D_0 = 12.0 ± 1.5 mm with a good correlation coefficient of R^2 = 0.91. The fitting parameter D_0 represents the sensitivity of the Lamb wave detection system. The smaller the D_0 is, the more sensitive the Lamb wave

detection system is for the small disbond defect. On the other hand, a larger D_0 value means the Lamb wave detection system can be effectively used to monitor a bigger disbond defect. The parameter D_0 is believed to rely on the structure of the GLARE composite as well as the configuration of the disbond defect and the Lamb wave transducers. Further research is needed to clarify the influence of these factors on the parameter D_0 as this is of critical significance to the application of the Lamb wave in structural health monitoring of the disbond defects.

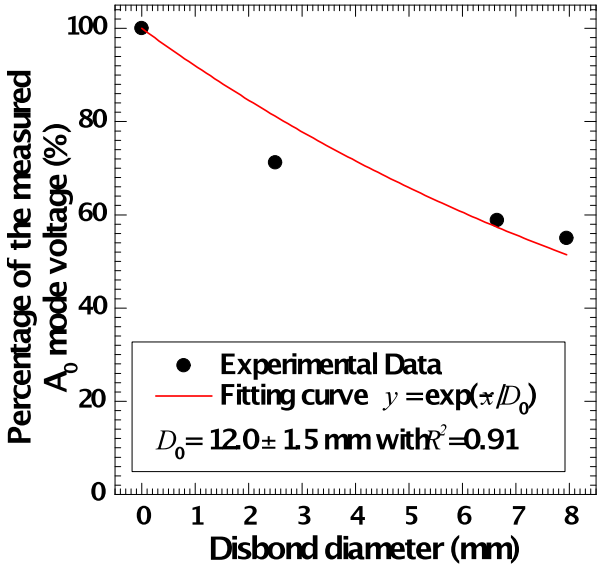

Figure 8: Percentage of the measured A_0 mode Lamb wave voltage as a function of the disbond diameter.

5. CONCLUSION

In summary, A FEM model was built to simulate the influence of a disbond on the lamb wave propagation. Both the displacement amplitudes and travel time of the A_o mode Lamb wave were shown to be influenced by the disbond void. For the void length less than 1

mm, the displacement amplitudes reduce with increasing the void size. This trend does not valid for the void length larger than 1.0mm. The time delay increases with increasing the disbond sizes, which can be used as the parameter to monitor a disbond defect growth in the GLARE plate. From the calculated result, the detectable disbond void size can be predicted as small as 0.1 mm at the selected frequency.

In experiments, a series of ball drops was used to introduce a disbond defect in the GLARE plate. The disbond defect was confirmed and measured with a thermal imaging system. Modally-selective guided Lamb waves were demonstrated to be launched successfully and were used to detect the disbond defect in the GLARE plate. The measured A_0 mode Lamb wave signals decrease linearly as a function of the ball impact events. By combining the thermal imaging results, the collected A_0 mode Lamb wave signals were found to decay exponentially with increasing disbond diameter. It is shown that the disbond defect sizes can be predicted from the measured Lamb wave signals using a simple exponential model.

ACKNOWLEDGEMENTS

This work is supported by the Federal Aviation Administration through the Joint Advanced Materials Center of Excellence program grant number 04-C-AM-NWU to Northwestern University.

REFERENCES

1. S. C. Rosalie, M. Vaughan, A. Bremner and W. K. Chiu, "Variation in the group velocity of lamb waves as a tool for the detection of delamination in glare aluminium plate-like structures," Composite Structures 66 (2004): 77-86.
2. G. C. Wu and J. M. Yang, "The mechanical behavior of glare laminates for aircraft structures," JOM 57 (2005): 72-79.
3. E. C. Botelho, R. A. Silva, L. C. Pardini and M. C. Rezende, "A review on the development and properties of continuous fiber/epoxy/aluminum hybrid composites for aircraft structures," Materials Research 9 (2006): 247-256.
4. C. Vermeeren, "An historic overview of the development of fibre metal laminates," Applied Composite Materials 10 (2003): 189-205.
5. A. Vlot, "Glare history of the development of a new aircraft material, Kluwer Academic Publishers, Dordrecht, The Netherlands, 2001.
6. R. L. Vijay Kumar, N. D. Jawali, L. Srikanth, C. Rahul Kumar, M. R. Prakash and R. M. V. G. K. Rao, "Post impact compression strength (pics) evaluation of glass/epoxy composite using a novel approach effect of delamination area," Journal of Reinforced Plastics and Composites 26 (2007): 1101-1109.
7. G. R. Kirikera, L. Sun, H. G. Kil, S. Krishnaswamy and J. D. Achenbach, "Matched ultrasonic transducers and assessment of transducer performance for robust structural health monitoring applications," Review of Progress in Quantitative Nondestructive Evaluation 27 (2008): 1436-1444.

8. T. Liu, M. Veidt and S. Kitipornchai, "Single mode lamb waves in composite laminated plates generated by piezoelectric transducers," Composite Structures 58 (2002): 381-396.
9. F. Bagnoli, M. Bernabei, D. Figueroa-Gordon and P. E. Irving, "The response of aluminium/glare hybrid materials to impact and to in-plane fatigue," Materials Science and Engineering A-Structural Materials Properties Microstructure and Processing 523 (2009): 118-124.
10. R. L. V. Kumar, N. D. Jawali, L. Srikanth, C. R. Kumar, M. R. Prakash and R. Rao, "Post impact compression strength (pics) evaluation of glass/epoxy composite using a novel approach - effect of delamination area," Journal Of Reinforced Plastics And Composites 26 (2007): 1101-1109.
11. C. R. Kumar, K. Radhakrishna and R. M. V. G. K. Rao, "Postcuring effects on impact behavior of glass/epoxy composite laminates," Journal of Reinforced Plastics and Composites 24 (2005): 949-960.
12. G. Petculescu, S. Krishnaswamy and J. D. Achenbach, "Group delay measurements using modally selective lamb wave transducers for detection and sizing of delaminations in composites," Smart Materials & Structures 17 (2008): 015007.
13. N. Hu, T. Shimomukai, C. Yan and H. Fukunaga, "Identification of delamination position in cross-ply laminated composite beams using s0 lamb mode," Composites Science and Technology 68 (2008): 1548-1554.
14. N. Guo and P. Cawley, "The interaction of lamb waves with delaminations in composite laminates," Journal of The Acoustical Society of America 94 (1993): 2240-2246.